ACS Chapter Nigeria Book of Proceedings 15th Annual Symposium
ISBN: 978-978-68-0485-9 DOI: https://doi.org/10.55455/acsnigeria.1.2.102-108

# Biological and Catalytic Activity of Biosynthesized Iron Nanoparticles (FeNPs) using Aqueous Extract from the Bark of *Antiaris toxicaria*

**Thomas Ndidi Asiwe, Atim Sunday Johnson, Idongesit Bassey Anweting and Simon Nzikahyel**
Department of Chemistry, University of Uyo, P.M.B 1017, Uyo, Nigeria **Corresponding Author's email:** michealasiwe@gmail.com

## ABSTRACT

Iron nanoparticles (FeNPs) were synthesized using *Antiaris toxicaria* bark extract as a reducing and stabilizing agent. The FeNPs were analyzed with UV-visible spectroscopy (UV-Vis), Fourier Transform Infrared Spectroscopy (FTIR), X-ray Powder Diffraction (XRD), scanning electron microscopy (SEM), Transmission Electron Microscopy (TEM) and Energy dispersive spectroscopy (EDS). The extract quickly reduced $Fe^{2+}$ to $Fe^{0}$, forming FeNPs (1–100 nm) with a face-centered cubic structure, confirmed by XRD. UV-Vis showed a surface plasmon resonance peak at 308 nm. FTIR peaks at 3296.3 $cm^{-1}$ (O–H group), 2165.78 $cm^{-1}$ ($CH_2$ stretching), and 1631.5 $cm^{-1}$ (C=O group) indicated the extract's role in FeNPs formation. The FeNPs showed strong antimicrobial activity, with a 30 mm inhibition zone against *Candida albicans* at 250 mg/mL, and high catalytic activity in degrading brilliant green dye.

**KEYWORDS:** Iron nanoparticles, *Antiaris toxicaria*, characterization, plant extract, brilliant green.

## 1. INTRODUCTION

Nanoparticles (NPs), which measure $10^{-9}$, exhibit properties very different from bulk materials due to their minute size and increased surface area [1]. They are categorized into two broad groups: organic nanoparticles, which includes fullerenes, and inorganic nanoparticles, including metals like iron and silver or metal oxides such as titanium dioxide [2,3]. As their size decreases, surface area-to-volume ratio increases, making them more chemically reactive. Through chemical modification, nanoparticles are stabilized in suspension, preventing agglomeration and enabling the usage in areas like cancer therapy, water treatment and biosensing [4]. Iron nanoparticles (FeNPs) are especially noteworthy for their strong magnetic behavior and reactivity, which make them useful in drug delivery, antimicrobial treatments, and pollutant degradation [5,4,6]. A sustainable way to produce such particles is green synthesis, that employs extract of plants, microbes, or algae as reducing and stabilizing agents. This method is not only cost-effective but also avoids toxic byproducts. Plant-derived compounds like flavonoids as well as phenols, in particular, play an important role in forming and stabilizing nanoparticles [7].

One promising source is *Antiaris toxicaria*, a tree native to Nigeria and Kenya. The tree bark is found of bioactive molecules like flavonoids, tannins and cardiac glycosides and has traditionally been employed in traditional medicine to relieve chest pain and support mental health [8]. While many other plants have been investigated for producing iron nanoparticles with antimicrobial or environmentalremediation properties, the bark of *A. toxicaria* remains underexplored. This study therefore investigates its use in fabricating FeNPs, characterizing them with UV–Vis, FTIR, XRD, TEM, SEM, and EDS, and evaluating its antimicrobial and catalytic activities. This study not only contributes to green nanotechnology but also highlights an overlooked natural resource with potential medical and environmental applications.

## 2. MATERIALS AND METHODS

### 2.1. Materials

Iron (II) chloride tetrahydrate ($FeCl_2.4H_2O$) (97.0%, SureChem), brilliant green (BG) (99.5%, JHD), and hydrogen peroxide ($H_2O_2$) (99.5%, JHD) were used, all analytical grade. Deionized water was used throughout. *Antiaris toxicaria* bark was collected from Ibiono, Akwa Ibom, Nigeria.

### 2.2. Extract Preparation

Bark of *A. toxicaria* was rinsed with tap and deionized water, cut and air-dried. Thirty grams (30 g) of powdered bark was boiled in 300 mL deionized water at 80°C for 30 minutes, cooled, and filtered through Whatman No. 1 paper to achieve the extract for nanoparticles synthesis.

### 2.3. Nanoparticle Synthesis

A modified method [9], 0.099 g $FeCl_2 \cdot 4H_2O$ was dissolved in 250 mL deionized water making a 0.001 M solution, heated at 60°C for 60 mins with stirring. 5 mL of the extract was mixed with 5 mL



precursor solution, stirred until the colour changed from light brown to black, indicating FeNPs formation. The nanoparticles were filtered, washed, oven-dried at 70°C for 2 hours, and stored sealed.

### 2.4. Characterization

The synthesized nanoparticles were analyzed using UV-Vis spectroscopy (Shimadzu UV-1800, 200–800 nm), FTIR (Perkin Elmer 1750) for functional groups, SEM (JEOL JSM-6610LV) with EDS for elemental composition, TEM (JEOL JEM-2100F, 200 kV) for size and morphology, and XRD (Rigaku Ultima IV, 4–90° 2θ) for crystallinity. Catalytic activity was evaluated with a Unicam Helios spectrophotometer.

### 2.5. Antimicrobial Activity

The extract and synthesized NPs were tested against *Salmonella* sp., *Staphylococcus aureus*, *Candida albicans*, *Pseudomonas aeruginosa*, and *Aspergillus flavus*. All the organisms were gotten from Department of Microbiology, University of Uyo. Using agar well diffusion, isolates were diluted ($10^3$ for Gram-positive/fungi, $10^5$ for Gram-negative), standardized to 0.5 McFarland (OD 0.008–0.1 at 600 nm), and 0.1 mL spread on Mueller-Hinton agar. 5 mm wells received 0.2 mL extract and FeNPs (150–250 mg/mL). Controls were chloramphenicol (25 mg/mL) and nystatin (40 mg/mL). Bacteria were incubated at 37°C for 24 hours, fungi at 28°C for 72 hours, and inhibition zones measured. MIC was determined by diluting samples, inoculating microbes, and noting the concentration at its lowest preventing growth after 24 to 48 hours.

### 2.6. Dye Reduction

Catalytic activity was tested by mixing 6 mL 0.1 mM BG with 4 mL 8 mM $H_2O_2$, measuring absorbance for 10 minutes. Another test combined 6 mL BG, 2 mL FeNP solution, and 2 mL $H_2O_2$, tracking absorbance with Genesys 50 UV-Vis spectrophotometer.

## 3. RESULTS AND DISCUSSION

### 3.1. UV-visible spectroscopy

A colour change of the solution from light brown to black within 60 mins, indicating FeNPs formation. This colour change is likely as a result of surface plasmon resonance (SPR) excitation in FeNPs, driven by the extract's phenolic compounds and Bioactive compounds which reduce iron ions into nanoparticles. UV-Vis spectroscopy confirmed FeNPs synthesis, showing a peak absorbance value at 308 nm (Figure 1), typical of iron's SPR in the ultraviolet region, consistent with reported absorbance at 289 to 320 nm in similar studies [10,11,12].

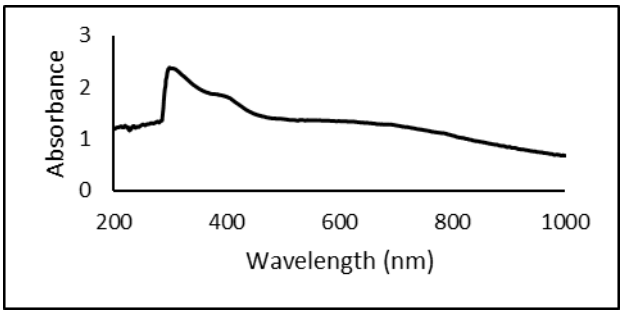


**Figure 1.** UV- visible spectrum of FeNPs **Source:** Field data

### 3.2. Energy Dispersive Spectroscopy (EDS) Analysis

The EDS analysis of the synthesized FeNPs, presented iron, oxygen, carbon, and silicon in their percentage composition (Figure 2). These extra elements likely result from the metabolites in the *A. toxicaria* extract employed in the synthesis. Similar results were noted [13] in their study of silver nanoparticles made with *Citrus reticulata* peel extract, where additional elements were also attributed to the plant's bioactive molecules.

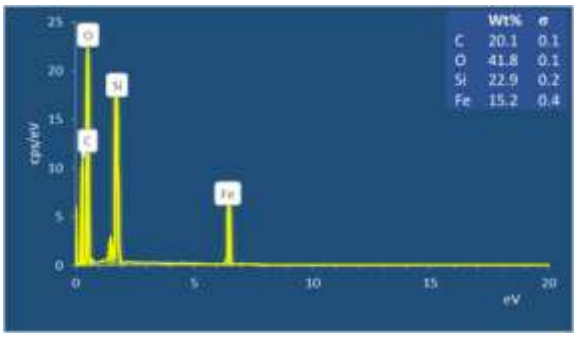


**Figure 2.** EDS of FeNPs **Source:** Field data

### 3.3. Fourier Transform-Infrared Radiation (FT-IR) Analysis

In FTIR spectra (Figure 3a for extract, 3b for FeNPs) showed peak shifts with $FeCl_2 \cdot 4H_2O$ to 425.92, 1631.5, 2165.8, and 3296.3 $cm^{-1}$. The extract's peak at 422.29 $cm^{-1}$ moved to 425.92 $cm^{-1}$, indicating an O–Fe–O network and ring-opening. A band at 1635.41 $cm^{-1}$ showed C=C stretching in aromatic rings, while 2165.8 $cm^{-1}$ indicated $CH_2$ as well as C-H alkane groups. O–H stretching in carboxylic acids shifted from 3325.35 $cm^{-1}$ to 3296.3 $cm^{-1}$, and peaks 402.66, 413.97, and 467.28 $cm^{-1}$ also shifted, suggesting ring-opening. Proteins and flavonoids likely reduced $Fe^{2+}$ to $Fe^0$ and capped the FeNPs, with flavonoids as primary reducing agents. **a**

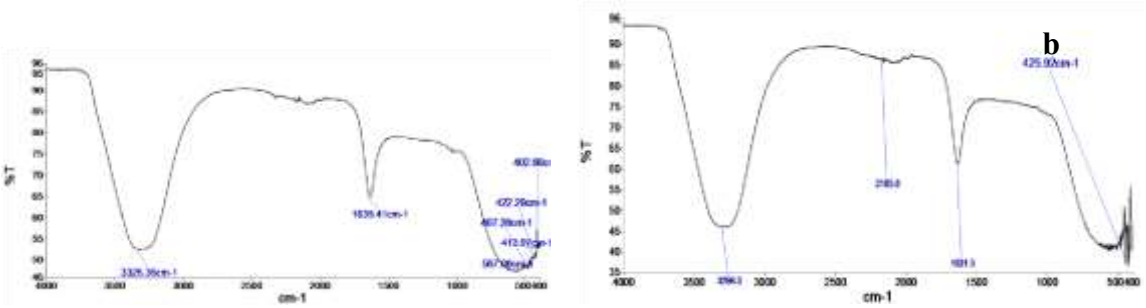


**Figure 3.** FT-IR spectrum of (a) bark *A. toxicaria* extract and (b) FeNPs **Source:** Field data

### 3.4. SEM and TEM Analysis

SEM images of the iron nanoparticles (FeNPs), revealed in Figure 4, reveal spherical particles with noticeable clustering, indicating some agglomeration. TEM images (Figure 5) confirm that the FeNPs are mostly spherical, well-dispersed, and homogeneous, though some have irregular shapes. Particle sizes, ranging up to 100 nm aligning with previous studies [14,15]

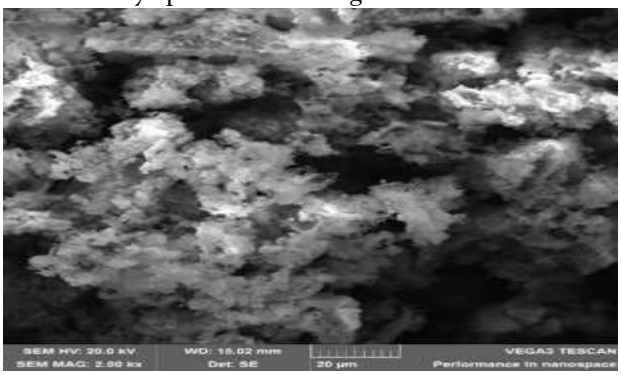

**Figure 4.** SEM image of FeNPs **Source:** Field data

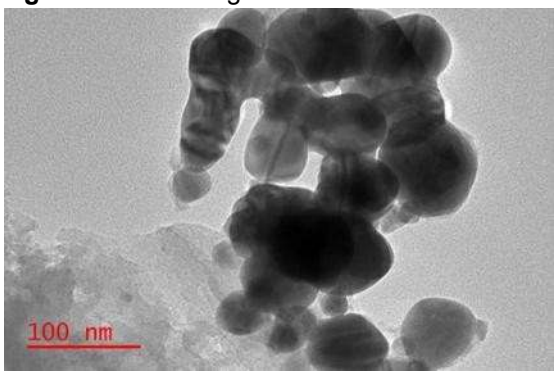


**Figure 5.** TEM image of FeNPs **Source:** Field data

### 3.5. X-ray Diffraction

The XRD pattern presents sharp peaks confirming the crystalline nature of the biosynthesized iron nanoparticles (FeNPs). Four distinct peaks at 2θ angles of 33.97°, 44.68°, 47.58°, and 57.4° match the (111), (200), (300), and (330) planes (Figure 6), indicating a face-centered cubic (fcc) structure for iron, consistent with prior studies [16,17]. These results verify the successful green synthesis and high purity of the FeNPs.

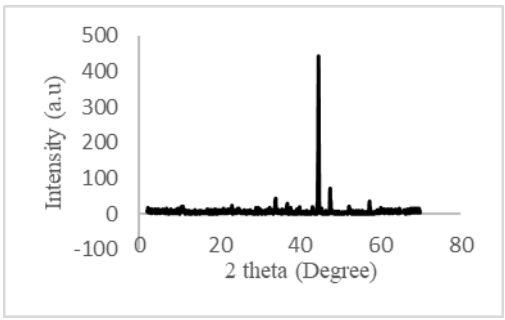


**Figure 6.** XRD pattern of FeNPs **Source:** Field data

### 3.6. Antimicrobial Studies

The bark extract of *A. toxicaria* and its iron nanoparticles (FeNPs) were tested for antimicrobial effects by measuring inhibition zones. Tables 1 present the antibacterial and antifungal activities at various concentrations. At 250 mg/mL, the extract inhibited *Staphylococcus aureus, Salmonella sp., Pseudomonas aeruginosa, Candida albicans,* and *Aspergillus flavus* with zones of 22 mm, 27 mm, 20 mm, 21 mm, and 24 mm, respectively. FeNPs showed zones of 28 mm, 23 mm, 20 mm, 30 mm, and 16 mm, respectively. Higher concentrations of both extract and FeNPs increased antimicrobial activity. The standard drug chloramphenicol showed stronger inhibition against bacteria (38 mm, 24 mm, 40 mm

for *S. aureus, Salmonella sp.,* and *P. aeruginosa*), while nystatin inhibited *C. albicans (33 mm) and A. flavus* (15 mm). Figure 7 shows the minimum inhibitory concentration (MIC) for both extract and FeNPs, with *S. aureus, C. albicans,* and *A. flavus* showing an MIC of 50 mg/mL. The results are consistent with reports from similar study [18] suggesting that both the extract and FeNPs effectively inhibit microbial growth, likely due to the extract's bioactive compounds and the nanoparticles' large surface area, which may disrupt bacterial cell membranes, increasing permeability and causing cell death.

**Table 1:** Antimicrobial activity with inhibition zones at different concentration of the bark extract of *A. toxicaria* and FeNPs against test organisms.

| Microorganism | Zones of Inhibition (mm) Concentration (mg/mL) A. toxicaria | | | FeNPs | | | Standard Chloramphenicol/ Nystatin |
|---|---|---|---|---|---|---|---|
| | 250 | 200 | 150 | 250 | 200 | 150 | |
| *Stahylococcus aureus* | 22 | 19 | 15 | 28 | 22 | 17 | 38 25/40 |
| *Salmonella sp* | 27 | 24 | 20 | 23 | 18 | 15 | 24 |
| *Pseudomonas aeruginosa* | 20 | 16 | 12 | 20 | 16 | 12 | 40 |
| *Candida albicans* | 21 | 16 | 13 | 30 | 26 | 22 | 33 |
| *Aspergillus flavus* | 24 | 18 | 14 | 16 | 12 | 9 | 15 |

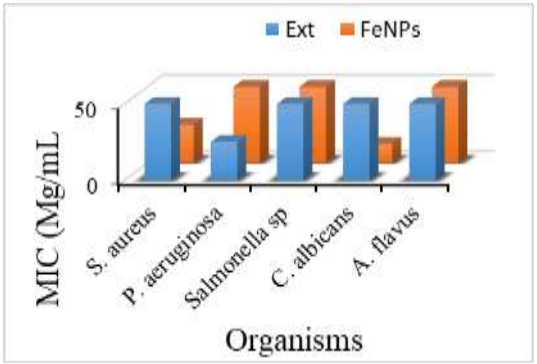


**Figure 7.** MIC of *A. toxicaria* extract and FeNPs **Source:** Field data

### 3.7. Catalytic activity of iron nanoparticles

Pure BG dye, with a λmax of 625 nm, changed from deep green to colorless over 10-minute intervals, indicating degradation (Figure 8). FeNPs facilitated this by acting as a redox catalyst, transferring electrons between hydrogen peroxide and BG. The absorption spectrum showed decreasing BG peaks and increasing FeNP peaks over time, with the dye's absorbance nearing baseline. UV spectra revealed an FeNP SPR band after 10 minutes (Figure 8a). Without FeNPs, $H_2O_2$ degraded BG slowly, with minimal absorbance reduction (Figure 8b). With FeNPs, absorbance dropped significantly, showing faster degradation. A plot of Log (At - A∞) versus time (Figure 9) indicated pseudo-first-order kinetics for BG degradation, given excess $H_2O_2$. The rate constant for $H_2O_2$ alone was 0.023 $min^{-1}$, while FeNPs increased it to 0.226 $min^{-1}$, demonstrating superior catalytic efficiency as similar report was reported [19]

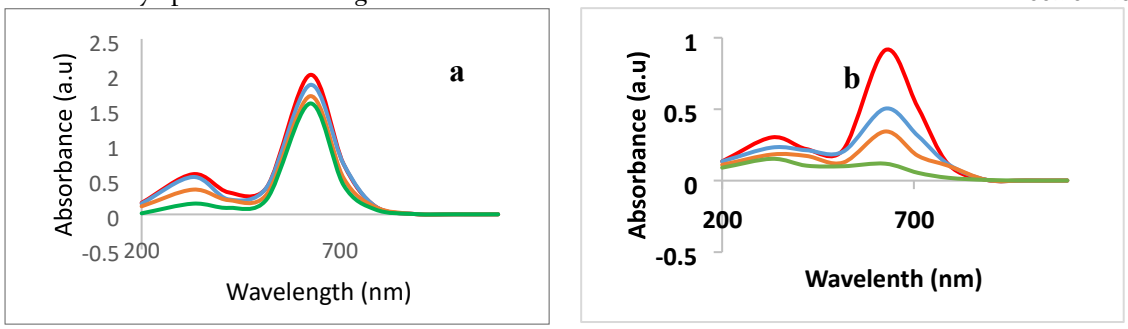


**Figure 8.** Reduction of BG dye with of $H_2O_2$ and (a) absence of FeNPs (b) presence of FeNPs
**Source: Field data**

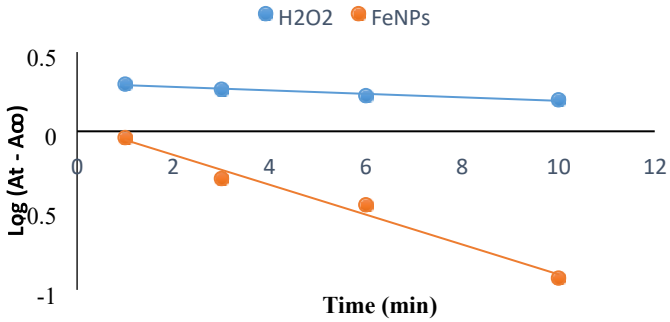


**Figure 9.** Plots for the degradation reaction of BG by $H_2O_2$ and FeNPs
**Source: Field data**

## 4. CONCLUSION

Iron nanoparticles were successfully synthesized using *A. toxicaria* bark extract, which served as both a reducing and stabilizing agent. The particles (1–100 nm) formed a stable cubic structure and showed strong antimicrobial activity, with a 30 mm inhibition zone against *Candida albicans*. They also degraded Brilliant Green dye effectively, highlighting their promise for both infection control and environmental cleanup. Further research is needed to fully explore their potential.

## ACKNOWLEDGEMENTS

We wish to sincerely appreciate the financial assistance granted us by the Tertiary Education Trust Fund (TETFUND) through the Management of the University of Uyo, Uyo for this research.

## CONFLICT OF INTERESTS

The authors declare no conflict of interests.

## REFERENCES

(1) Khan, I.; Saeed, K.; Khan, I. Nanoparticles: Properties, Applications and Toxicities. *Arab. J. Chem.* **2019**, *12* (7), 908–931.

(2) Johnson, A.; Uwa, P. Eco-Friendly Synthesis of Iron Nanoparticles Using *Uvaria chamae*: Characterisation and Biological Activity. *Inorg. Nano-Met. Chem.* **2019**, 49 (12), 431–442.

(3) Ituen, E.; Ekemini, E.; Yuanhua, L.; Singh, A. Green Synthesis of *Citrus reticulata* Peels Extract Silver Nanoparticles and Characterisation of Structural, Biocide and Anticorrosion Properties. *J. Mol. Struct.* **2020**, *1207*, 127819.

(4) Abdellatif, A. A. H.; Alturki, H. N. H.; Tawfeek, H. M. Different Cellulosic Polymers for Synthesising Silver Nanoparticles with Antioxidant and Antibacterial Activities. *Sci. Rep.* **2021**, *11* (1), 84.

(5) Sandhu, Z. A.; Raza, M. A.; Alqurashi, A.; Sajid, S.; Ashraf, S.; Imtiaz, K.; Latif, M. Advances in the Optimization of Fe Nanoparticles: Unlocking Antifungal Properties for Biomedical Applications. *Pharmaceutics* **2024**, *16* (5), 645.

(6) Hariharan, K.; Patel, P.; Mehta, T. Surface Modifications of Gold Nanoparticles: Stabilization and Recent Applications in Cancer Therapy. *Pharm. Dev. Technol.* **2022**, *27* (6), 665–683.

(7) Santhosh, P. B.; Genova, J.; Chamati, H. Green Synthesis of Gold Nanoparticles: An Eco-Friendly Approach. *Chemistry* **2022**, *4* (2), 345–369.

(8) Umdale, S.; Mirgal, A.; Gaikwad, N. Phytoconstituents, Medicinal Uses and Conservation of Upastree (*Antiaris toxicaria* Lesch). In Biodiversity and Genetic Improvement of Medicinal and Aromatic Plants II; Springer Nature Switzerland: *Cham*, **2025**; pp 269–284.

(9) Asiwe, T. N.; Anweting, I. B.; Johnson, A. S.; Simon, N.; Shaibu, S. E. Eco-Friendly Synthesis and Characterization of Silver and Zinc Nanoparticles Using Aqueous Extract from the Bark of *Antiaris toxicaria*. *Commun. Phys. Sci.* **2024**, *12* (1), 149–161.

(10) Khan, Y.; Sadia, H.; Ali Shah, S. Z.; Khan, M. N.; Shah, A. A.; Ullah, N.; Khan, M. I. Classification, Synthetic, and Characterization Approaches to Nanoparticles, and Their Applications in Various Fields of Nanotechnology: A Review. *Catalysts* **2022**, *12* (11), 1386.

(11) Subiono, T.; Tavip, M. A. Qualitative and Quantitative Phytochemicals of Leaves, Bark and Roots of *Antiaris toxicaria* Lesch., a Promising Natural Medicinal Plant and Source of Pesticides. *Plant Sci. Today* **2023**, *10* (1), 5–10.

(12) Alsailawi, H. A.; Mudhafar, M.; Hanan, A. H.; Ayat, S. S.; Dhahi, S. J.; Ruaa, K. M.; Raheem, H. A. Phytochemical Screening and Antibacterial Activities of *Antiaris toxicaria* Stem, *Polyalthia rumphii* Leaves and *Polyalthia bullata* Stem Extracts. *AIP Conf. Proc.* **2023**, *2845* (1), AIP Publishing, September.

(13) Rizwan, M.; Shoukat, A.; Ayub, A.; Razzaq, B.; Tahir, M. B. Types and Classification of Nanomaterials. In Nanomaterials: Synthesis, Characterization, Hazards and Safety; *Elsevier*, 2021; pp 31-54

(14) Aderolu, H. A.; Aboaba, O. O.; Aderolu, A. Z.; Abdulwahab, K. O.; Suliman, A. A.; Emmanuel, U. C. Biological Synthesis of Copper Nanoparticles and Its Antimicrobial Potential on Selected Bacteria FoodBorne Pathogens. *Ife J. Sci.* 2021, 23 (1), 11–21.

(15) Borah, R.; Ag, K. R.; Minja, A. C.; Verbruggen, S. W. A Review on Self-Assembly of Colloidal Nanoparticles into Clusters, Patterns, and Films: Emerging Synthesis Techniques and Applications. *Small Methods* **2023**, 7 (6), 2201536.

(16) Sreelekha, E.; George, B.; Shyam, A.; Sajina, N.; Mathew, B. A Comparative Study on the Synthesis, Characterisation, and Antioxidant Activity of Green and Chemically Synthesised Silver Nanoparticles. *BioNanoScience* **2021**, *11*, 489–496.